



Zinc oxide nanoparticles and L-carnitine effects on neuro-schistosomiasis mansoni induced in mice

Amira A. Bauomy^{1,2}

Received: 25 September 2019 / Accepted: 6 March 2020 / Published online: 23 March 2020
© Springer-Verlag GmbH Germany, part of Springer Nature 2020

Abstract

Neuro-schistosomiasis can induce neurological symptoms and severe disability. Since the resistance against the chemotherapy “praziquantel” was reported, the aim of the present study was investigating the anti-neuro-schistosomal effects of ZnO nanoparticles and/or L-carnitine (as free radicals scavenger) on schistosome-infected mice, where technology of nanoparticles has come to the forefront in the medical diagnosis and therapeutic drug delivery. In the human body, nanoscale-sized particles can move freely and reveal unique biological, mechanical, electrical, and chemical properties. In the present study, mice were divided into five groups. The first group served as the non-infected control group. Groups II, III, IV, and V were infected with cercariae of *Schistosoma mansoni*. Mice of groups III and IV were treated with ZnO nanoparticles (5.6 mg/kg b. wt.) and L-carnitine (500 mg/kg b. wt.), respectively, after 47 days post-infection. Finally, mice of the fifth group were injected with ZnO nanoparticles and after 1 h, the mice were intraperitoneally injected with L-carnitine once daily for 5 days. On day 52, post-infection mice of all groups were cervically decapitated. The treatment of ZnO nanoparticles and/or L-carnitine to schistosome-infected mice decreased brain oxidative stress parameters, where glutathione level and catalase activity were significantly increased as compared to schistosome-infected group. On the contrary, the treatment decreased nitrite/nitrate, malondialdehyde, and reactive oxygen species levels significantly. In addition, ZnO nanoparticles and/or L-carnitine treatment restored DNA laddering profile and improved the brain histopathological impairments resulting from neuro-schistosomiasis. Finally, the ZnO nanoparticle treatment and the co-treatment of ZnO nanoparticles and L-carnitine revealed anti-neuro-schistosomal effects on the infected mice.

Keywords Neuro-schistosomiasis mansoni · ZnO nanoparticles · Oxidative stress · Histopathology · DNA fragmentation · Mice

Introduction

Neuro-schistosomiasis is a central nervous system disease affecting the brain or the spinal cord (Coyle 2013). *Schistosoma mansoni*, *S. haematobium*, or *S. japonicum* accounts for most cases of neuro-schistosomiasis, and many reports concluded

that *S. mansoni* induced cerebellar schistosomiasis (Braga et al. 2003; Raso et al. 2006). Chronic schistosomiasis results from the host’s immune response to the eggs lodged in the central nervous system which prompts granulomatous reaction and fibro-obstructive disease (Ranasinghe et al. 2018; Abdelgelil et al. 2019).

The most common manifestations of the disease are headache, motor deficits, visual abnormalities, seizures, altered mental status, sensory impairment, speech disturbances, and ataxia (Pittella et al. 1996; Ferrari et al. 2011). Infection with *S. mansoni* may cause a tumor-like mass in any of the brain lobes due to slowly expanding cerebral lesion; the most common sites of the tumor are the cerebellum and the occipital and frontal lobes (Ferrari et al. 2008).

Praziquantel is a broad-spectrum schistosomicidal drug that kills the adult female worms, resulting in a parasitological cure in 70–90% of patients (Saconato and Atallah 2000). However, in some African countries, the parasite has shown resistance against praziquantel (Coyle 2013).

Responsible editor: Mohamed M. Abdel-Daim

Electronic supplementary material The online version of this article (<https://doi.org/10.1007/s11356-020-08356-5>) contains supplementary material, which is available to authorized users.

✉ Amira A. Bauomy
Am.Mohamed@qu.edu.sa; amiraanwar1@gmail.com

¹ Department of Laboratory Sciences, College of Science & Arts, Al-Rass, Qassim University, Al-Rass 51921, Saudi Arabia

² Department of Zoology and Entomology, Faculty of Science, Helwan University, Ain Helwan, 11795, Egypt

Therefore, the development of effective alternative drug is important and can be achieved by nanoparticle-based drug formulations.

According to Abaza (2016), the principles of nanotechnology and applications of nanomaterials in medicine and techniques were discussed; moreover, nanoparticles were used to diagnose malaria, toxoplasmosis, leishmaniasis, and schistosomiasis mansoni.

It was reported that zinc oxide nanoparticles (ZnONPs) are present in sunscreens and cosmetic products due to their role in preventing skin cancers by protection from ultraviolet light and promoting pH balance and flora regeneration (Frederickson et al. 2005). Likewise, the Food and Drug Administration reported that ZnONPs are non-toxic to human (Emamifar et al. 2010). Additionally, zinc is an important element for human health; it is used in medicinal skin cream from 2000 BC, as mentioned in Egyptian papyri (Frederickson et al. 2005; Emamifar et al. 2010).

The nanosize of ZnO gives a higher exposure surface of the atoms on nanoparticles, thus exhibiting different physical, chemical, and very high level of biological responses (Khan et al. 2015). In the same manner, Chitra and Annadurai (2013) reported that ZnONPs have a good biocompatibility with the human cells and have antibacterial activity. In piglets, ZnONPs acted as antimicrobial and immune-modulatory agent, where it reduced the rate of diarrhea (Hongfu 2008). In addition, Ahmadi et al. (2014) recorded that the dietary ZnONPs improved the oxidant state and had positive effect on several serum enzymes activity. Therefore, ZnONPs have been used as a novel therapy against *Leishmania* (Nadhman et al. 2014).

L-Carnitine (L-Carnt) is an L-lysine derivative (3-hydroxy-4-N-trimethylammonio-butanoate). Red meat and milk diet is the main source of L-Carnt (Brevetti and Perna 1992; Alzoubi et al. 2017). In the mammalians' kidney, liver, muscles, and brain, L-Carnt is synthesized from the essential amino acids lysine and methionine (Pettegrew et al. 2000). According to Tamai (2013), L-Carnt is taken into the cells by organic cation transporters that act as endogenous substrates and L-Carnt transporters. These transporters are localized in different organs of human and rats, such as the brain, heart, intestine, kidney, liver, lung, pancreas, placenta, thyroid, and trachea. Across the mitochondria, L-Carnt acts as a mediator of long-chain fatty acid transport to facilitate β -oxidation cycle, and it has shown antioxidant activities against reactive oxygen species (ROS) produced in the body (Rani and Panneerselvam 2002; Alzoubi et al. 2017).

Consequently, the aim of the present study is investigating the neuro-anti-schistosomal effects of ZnONPs or/and L-Carnt on infected mice with *S. mansoni*.

Materials and methods

Characterization of ZnONPs

ZnONPs, white powder, were purchased from International CO. for Scientific and Medical Supplies, Cairo, Egypt. According to Dkhil et al. (2015a), the ZnONP sample was characterized at room temperature (25 ± 1 °C) with transmission electron microscopy (TEM) equipped with a high resolution at an accelerating voltage of 200 kV (JEOL JEM-2100, JEOL Ltd., Tokyo, Japan). In ethanol, the nanostructures of white ZnONP powder was sonicated for 10–15 min, then a carbon-coated copper grid (400 mesh) was dipped in the suspension solution of nanoparticles and dried at room temperature (25 ± 1 °C), to analyze the crystallinity and structural morphology at 200 kV.

Animals and neuro-schistosomiasis infection

Forty-five male Swiss albino mice (9 to 11 weeks, weighing 20–25 g) were bred under specified pathogen-free conditions in the Schistosome Biological Supply Center at the Theodor Bilharz Research Institute, Imbaba, Giza, Egypt. Mice were fed a standard diet; water and diet were provided ad libitum. The experiments were approved by state authorities and followed Egyptian rules for animal protection. From the Theodor Bilharz Research Institute, *S. mansoni* cercariae were obtained and mice were infected subcutaneously by 100 ± 10 cercariae (Oliver and Stirewalt 1952).

Nanoparticles ZnO injection

ZnONPs were intraperitoneally (i.p.) injected to schistosome-infected mice for 5 days at a dose level of 5.6 mg/kg (Xie et al. 2012). A stock solution was prepared by dissolving 0.756 mg of ZnO nanoparticles in 5.4 ml (0.9%) normal saline and stored at 5 °C for daily injection.

L-Carnitine preparation

L-Carnt was purchased from a local pharmacy in Cairo. According to Yapar et al. (2007), L-Carnt was i.p. injected to schistosome-infected mice at a dose level of 500 mg/kg b. wt for 5 consecutive days.

Experimental design

Animals were divided into five groups. Nine mice are in each group. The non-infected mice served as the control (group I), where each mouse was i.p. injected (100 μ l—0.9% saline) for 5 days. Groups II, III, IV, and V were subcutaneously infected with 100 ± 10 *S. mansoni* cercariae. The animals of groups III and IV were i.p. injected with 100 μ l ZnONPs (5.6 mg/kg b.

wt.) and L-Carnt (500 mg/kg b. wt.), respectively, after 47 days post-infection (p.i.). Finally, the animals of the 5th group were i.p. injected with ZnONPs and after 1 h, the mice were i.p. injected with L-Carnt once daily for 5 days. On day 52, p.i. with *S. mansoni*, the animals of all groups were cervically decapitated.

Brain tissue preparations

After fast cervical decapitation, the brains were rapidly excised from the skulls and blotted with a filter paper. Then, the brains were weighed and wrapped in plastic films and quickly stored at -70°C until used for biochemical investigations.

The markers of the oxidative stress were estimated in the brains of six mice. Consecutively, the brains of the remaining three mice were used for histopathological investigations.

Brain oxidative stress estimation

To estimate the markers of brain oxidative stress, the brains were homogenized in ice-cold medium containing 50 mM Tris-HCl and 300 mM sucrose, at pH 7.4 (Tsakiris et al. 2004).

A reduced glutathione (GSH) level was determined in brain homogenates. The method is based on the reduction of Ellman's reagent (5,5'-dithiobis (2-nitrobenzoic acid)) with sample GSH to produce a yellow compound. The chromogen is directly proportional to the GSH concentration and its absorbance was measured at 405 nm (Ellman 1959).

To determine the activity of catalase (CAT), CAT reacts with a known quantity of hydrogen peroxide. Exactly after 1 min of catalase inhibitor addition, the reaction between CAT and hydrogen peroxide is stopped. In the presence of peroxidase, the remaining hydrogen peroxide reacts with 3,5-dichloro-2-hydroxybenzene sulfonic acid and 4-aminophenazone to form a chromophore with color intensity inversely proportional to the CAT activity in the brain homogenate samples (Aebi 1984).

The level of nitrite/nitrate was determined, according to the method of Green et al. (1982), where nitrous acid diazotize sulfanilamide was formed in an acid medium and in the presence of nitrite. Then, nitrous acid diazotize sulfanilamide is coupled with *N*-(1-naphthyl)ethylenediamine forming azo dye (a bright reddish purple color) and it can be measured at 540 nm.

The malondialdehyde (MDA) level was estimated in brain homogenate, where trichloroacetic acid (1 ml, 10%) and thiobarbituric acid (1 ml, 0.67%) were mixed and heated for 30 min in a boiling water bath. Thiobarbituric acid-reactive substances were measured at 535 nm (Ohkawa et al. 1979).

The generation of reactive oxygen species (ROS) was determined according to Vrablic et al. (2001), which is based on the intracellular conversion of nitro blue tetrazolium (NBT)

into formazan by superoxide anion. Briefly, 200 μl (1.0 mg/ml) NBT was added to the brain homogenate, and after 1 h of incubation at 37°C , solutions were treated with 100 μl (2 M) KOH. NBT reduced per gram of tissue expressed in nanomole was determined by spectrophotometry at 560 nm. If radical scavenging compounds were present in the tissue, less formazan blue would be formed.

DNA fragmentation assay

The DNA fragmentation assay was done by using agarose gel electrophoresis. Firstly, DNA was extracted according to Aljanabi and Martinez (1997); in Eppendorf tubes, brain tissue (20 mg) was lysed with 600 μl buffer (50 mM NaCl, 1 mM Na₂EDTA, 0.5% SDS, pH 8.3) and gently shaken. Overnight, the mixture was incubated at 37°C , and then 20 μl of saturated NaCl was added. The sample was shaken and centrifuged for 10 min, at 12,000 rpm. Thereafter, the supernatant was transferred to new Eppendorf tubes and cold isopropanol (600 μl) was added to precipitate DNA. The mixture was inverted several times until fine fibers appeared, and the Eppendorf tubes were centrifuged at 12,000 rpm, for 5 min. After removing the supernatant, the pellets were washed with ethyl alcohol (500 μl 70%) then centrifuged (12,000 rpm, 5 min); after centrifugation, the ethyl alcohol was decanted. On a Whatman filter paper, all tubes were plotted to dry. The pellets were re-suspended in 50 μl or appropriate volume of TE buffer (10 mM Tris, 1 mM EDTA, pH 8). The re-suspended DNA was incubated for 30–60 min with loading mix (RNase + loading buffer) and then loaded into the gel wells. The gel was prepared with agarose (2%) containing 0.1% ethidium bromide (200 $\mu\text{g}/\text{ml}$). The samples of DNA were mixed with loading buffer (0.25% bromophenol blue, 0.25% xylene cyanol FF and 30% glycerol) and loaded into the 20 μl wells of DNA/lane with a standard molecular-sized ladder marker (Pharmacia Biotech., USA). At a current of 50 mA for 1.5 h, the gel was electrophoresed using a submarine gel electrophoresis machine. Finally, with illumination under UV light, the DNA was visualized and photographed.

Brain index

At the end of the experimental period, each mouse was weighed and the weight of the brains was recorded after removing the brains from the skulls. The brain index was calculated as ratio of brain weight (mg) to mice body weight (g). Also, the percentage change was calculated as:

$$\% \text{Change} = \frac{\text{Mean of treated} - \text{Mean of infected control}}{\text{Mean of infected control}} \times 100$$

Histopathological investigations

After a fast cervical decapitation, brain tissue samples for 3 mice from each group were immediately fixed in 10% neutral buffered formalin, then dehydrated and processed for paraffin sectioning. Sections were then de-paraffinized and stained with hematoxylin and eosin (Slaoui and Fiette 2011).

Statistical analysis

The obtained data were presented as means \pm standard error. The statistical comparisons among the groups were fulfilled by using a one-way ANOVA which was performed with Duncan's test using a statistical package program (SPSS version 17.0). $P < 0.05$ was considered as low, moderate, and highly significant for all statistical analyses in this study.

Results

TEM for ZnONPs showed that the size of NPs was 25–40 nm, with a spherical shape and smooth surfaces (Fig. 1). The schistosome-infected mice revealed a significant reduction in the brain GSH level and CAT activity. Injection of ZnONPs to the schistosome-infected mice caused a significant decrease in the level of GSH and activity of CAT as compared with the non-infected control group. On the other hand, ZnONP treatment increased the GSH level and CAT activity in the brain of infected mice recording 61.83% and 56.83%, respectively, as a percentage change versus the corresponding infected group (Table 1).

L-Carnt treatment of the schistosome-infected mice showed a significant reduction ($P < 0.05$) in GSH level as compared with the non-infected control group. However, in comparison with the schistosome-infected mice (group II), L-Carnt injection caused a significant increase in the brain GSH level (83.79%) and CAT activity (254.3%). Moreover, ZnONP and L-Carnt co-treatment of the infected mice resulted in a

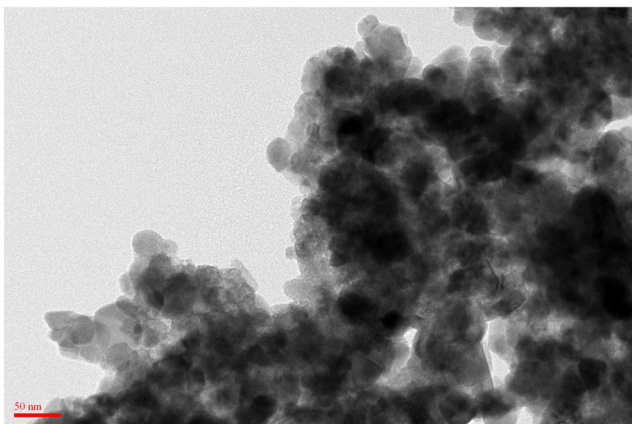


Fig. 1 A transmission electron microscopy (TEM) image of the ZnONPs illustrates their shape and size

significant raise in the brain GSH level and CAT activity with the percentage change of 141.7% and 288.7%, respectively, as compared with the infected group. A non-significant change was observed in the GSH level and CAT activity as a result of ZnONP and L-Carnt treatment of the infected mice as compared with the non-infected control group (Table 1).

A significant elevation was found in the levels of nitrite/nitrate, MDA, and ROS as a result of schistosomiasis infection versus the non-infected control group. The infected mice treated with ZnONPs showed a significant increase in ROS levels as compared with the non-infected control group. Oppositely, in a comparison with the schistosome-infected mice, a significant decrease was observed in levels of nitrite/nitrate, MDA, and ROS as a result of ZnONP treatment of the infected group recording -31.90% , -39.48% , and -13.33% , respectively, as the percentage change (Table 1).

A non-significant increase was found in the nitrite/nitrate and MDA levels as a result of L-Carnt injection to the schistosome-infected mice, while the ROS level showed a significant increase as compared with that of the non-infected control group. Meanwhile, in comparison with the infected group, treatment of schistosome-infected mice with L-Carnt induced a significant reduction in all levels of nitrite/nitrate, MDA, and ROS recording -37.40% , -46.86% , and -55.00% , respectively, as the percentage change (Table 1).

Treatment of the schistosome-infected mice with both ZnONPs and L-Carnt revealed a significant increase in brain nitrite/nitrate and ROS levels versus that of the non-infected control group. However, a non-significant change was recorded in MDA level as a result of ZnONP and L-Carnt treatment to infected mice. On the other hand, a significant reduction was obtained in the levels of brain nitrite/nitrate, MDA, and ROS as a result of ZnONP and L-Carnt co-treatment of the infected mice with the percentage change -28.58% , -50.15% , and -45.00% , respectively, as compared with that of the schistosome-infected group (Table 1).

The parasite infection induced apoptotic DNA fragmentation in the brain of mice, where the apoptotic DNA fragmentation was clearly indicated on the agarose gel as detected by ethidium bromide fluorescence (Fig. 2); the raw data are showed in Supplementary Fig. 1. However, the DNA of normal brain tissue showed no ladder (Fig. 2, lane 1). A genomic DNA ladder was formed and observed in mice infected with *S. mansoni* (Fig. 2, lane 2). Moreover, ZnONP treatment of the schistosome-infected mice showed a partial DNA fragmentation (lane 3). Treatment of infected mice with L-Carnt alone and with nanoZnO and L-Carnt (Fig. 2, lanes 4 and 5, respectively) restored the DNA laddering profile induced by schistosomiasis mansoni.

Mice infected with the parasite showed significant histopathological impairments which induced nuclear pyknosis, vacuolization, and brain edema. The brain of infected mice showed vascular cognition as well (Fig. 3b). Finally, the last

Table 1 Changes of oxidative stress markers in the brain of the schistosomiasis-infected mice treated with ZnONPs and/or L-Carnt

Group	GSH (mg/g)	CAT (U/g)	Nitrite/nitrate (μmol/g)	MDA (nmol/g)	ROS (μmol/g)
Non-infected	12.97 ± 0.74	1019.2 ± 44.1	70.19 ± 2.76	23.52 ± 1.10	0.06 ± 0.004
Infected	04.69 ± 0.23 ^a	273.6 ± 9.99 ^a	116.3 ± 4.09 ^a	49.31 ± 2.32 ^a	0.60 ± 0.02 ^a
Infected (+ nanoZnO)	07.59 ± 0.38 ^{ab} (61.83%)	429.1 ± 19.1 ^{ab} (56.83%)	79.19 ± 3.24 ^b (-31.90%)	29.84 ± 1.14 ^b (-39.48%)	0.52 ± 0.03 ^{ab} (-13.33%)
Infected (+ L-carnitine)	08.62 ± 0.54 ^{ab} (83.79%)	969.5 ± 41.6 ^b (254.3%)	72.80 ± 3.48 ^b (-46.86%)	26.20 ± 0.74 ^b (-46.86%)	0.27 ± 0.01 ^{ab} (-55.00%)
Infected (+ nanoZnO and L-carnitine)	11.34 ± 0.43 ^b (141.7%)	1063.6 ± 31.7 ^b (288.7%)	83.05 ± 3.45 ^{ab} (-28.58%)	24.58 ± 1.57 ^b (-50.15%)	0.33 ± 0.02 ^{ab} (-45.00%)

Values are means ± SE

Values of the percentage change (%) with respect to infected control value, *n* = 6

^a Significant against non-infected control group at *P* ≤ 0.05

^b Significant against infected control group at *P* ≤ 0.05

three schistosomiasis-infected groups that were treated with ZnONPs, L-Carnt, and ZnONPs and L-Carnt showed improvements in the brain histological picture as compared with both the infected group and the non-infected control group, respectively (Fig. 3c–e).

As shown in Fig. 4, the calculation of the brain index showed a non-significant change in the infected group as compared with that in the non-infected control group. Likewise, a non-significant change was found in the brain index of the infected mice treated with ZnONPs or/and L-Carnt versus the control group. However, a significant increase was recorded in the brain index of the schistosomiasis-infected mice treated with L-Carnt compared with that of the infected group.

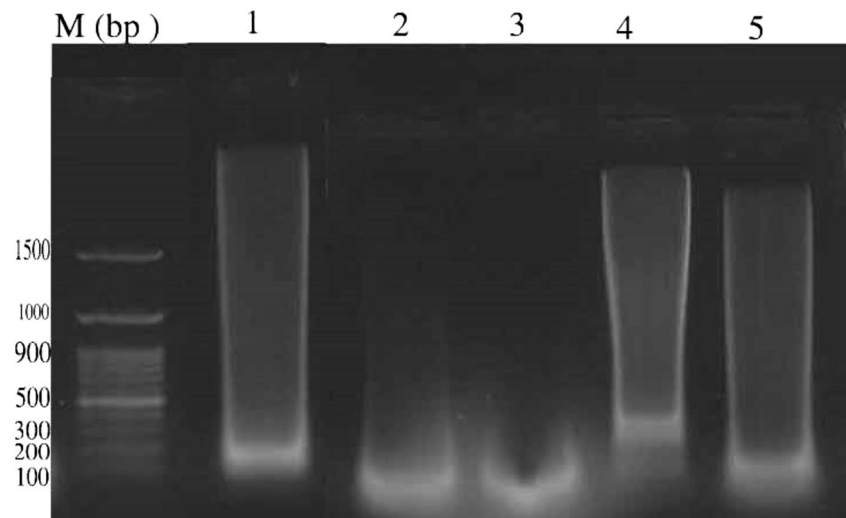
Discussion

ZnONPs are the third highest globally produced nanometals after SiO₂ and TiO₂ nanoparticles (Piccinno et al. 2011). In an animal body, nanominerals interact more effectively with organic and inorganic substances due to their larger surface area (Zaboli et al. 2013). Moreover, atoms of ZnO nanoparticles give a higher surface exposure, thereby exhibiting different physical, chemical, and a very high level of biological responses (Wahab et al. 2010; Jin et al. 2014). All the characteristics of the ZnONPs such as absorption and distribution depend on some factors like the size and shape of particles, where the decreased size is more effective (Siddiqi et al. 2018). Additionally, it was reported that ZnONPs have minimal or no adverse effects on the human cells, but is toxic to the microorganisms (Reddy et al. 2007; Chitra and Annadurai 2013).

In the present results, neuro-schistosomiasis increased MDA, nitrite/nitrate, and ROS levels significantly in the brain tissues; however, the GSH level and CAT activity showed a significant decrease versus the non-infected control group. Moreover, treatment of neuro-schistosomiasis by ZnONPs or/and L-Carnt showed a significant decrease in MDA, nitrite/nitrate, and ROS levels; in addition, a significant increase of the GSH level and CAT activity in brain homogenate was recorded as compared with the infected group. These results are in agreement with many studies (Rani and Panneerselvam 2002; Chitra and Annadurai 2013; de Oliveira et al. 2013; Bauomy 2014; Dkhil et al. 2015a, b; Nazarizadeh and Asri-Rezaie 2016; Alzoubi et al. 2017).

According to de Oliveira et al. (2013), schistosomiasis mansoni-infected mice altered the non-enzymatic antioxidant status in the brain. Likewise, Bauomy (2014) and Dkhil et al. (2015b) demonstrated that neuro-schistosomiasis induced a significant imbalance in the non-enzymatic and enzymatic antioxidants. GSH, total antioxidant capacity, level and CAT activity showed a marked reduction in brain tissue of the infected mice. On the contrary, MDA and nitrite/nitrate levels showed a significant increment versus the non-infected group.

Fig. 2 Effect of ZnONPs and/or L-Camt treatment in the schistosome-infected mice on agarose gel electrophoresis photograph of DNA extracted from brain tissue of normal and treated mice. M, marker. Lane 1—normal control group showed no DNA laddering; lane 2—schistosome mansoni–infected (Inf) group showed DNA laddering band; lane 3—Inf + ZnONPs group showed a partial laddering band; and lanes 4 and 5—Inf + L-Camt– and Inf + ZnONPs + L-Camt–treated groups, respectively—restored DNA laddering



In pathogens, ZnONPs exhibit a strong tendency to generate ROS and oxidative stress; thus, they are used as antibacterial agents (Yu et al. 2013). Abdel-Daim et al. (2019) reported that the spherical and rod shape of ZnONPs (size ≤ 100 nm) at a dose 50 mg/l for 30 days increased the MDA level in serum, the liver, and the kidney of Nile tilapia, but decreased the GSH level and SOD activity. Moreover, Kirthi et al. (2011) was the first who reported on the anti-parasitic activity of the synthesized ZnONPs. Likewise, Gandhi et al. (2017) concluded that synthesized ZnONPs possess excellent anti-parasitic activity, and in the same manner, Dkhil et al. (2015a) reported that the nanoparticles of ZnO revealed anticoccidial and antioxidant activities. Khan et al. (2015) and Nazarizadeh

and Asri-Rezaie (2016) decided that in vitro ZnONPs increased ROS, MDA, and nitric oxide levels that induced the oxidative stress in *Gigantocotyle explanatum* and *Toxocara vitulorum*; the authors attributed that the generated oxidative stress targets the lipids that initiate lipid peroxidation in the parasite organelles and macromolecules like nucleic acids and protein, and consequently, the contractile movement of worms was affected by ZnONPs.

Additionally, Sabir et al. (2014) and Nazarizadeh and Asri-Rezaie (2016) concluded that ZnONPs exert anthelmintic and antibacterial effects via induction of oxidative/nitrosative stress. Finally, Khan et al. (2015) reported that several kinds of nanoparticles have been proposed as anti-parasite agents. In

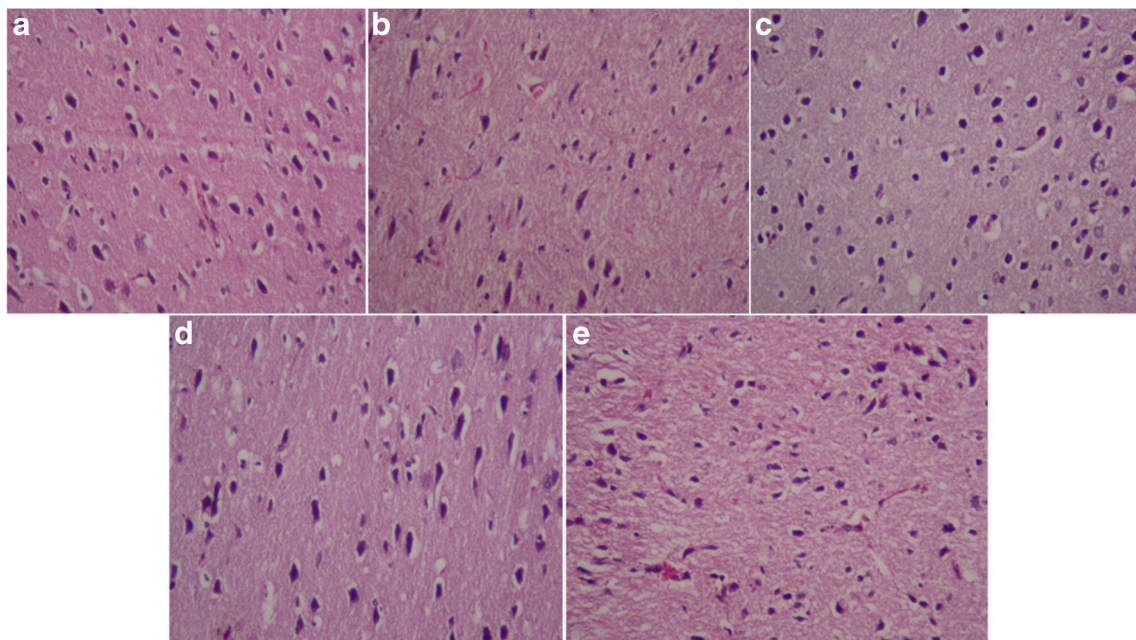
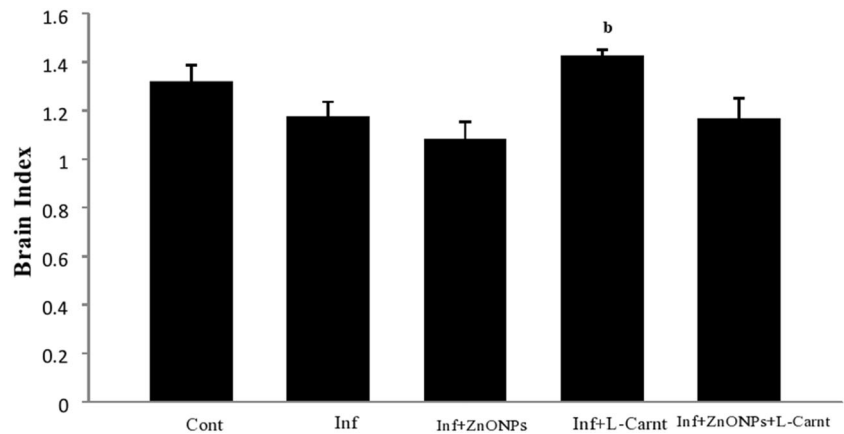


Fig. 3 Histological picture of mice brain infected with *S. mansoni* on day 47 p.i. **a** Non-infected brain tissue. **b** Infected brain with schistosomiasis mansoni. **c** Brain of schistosome-infected mice treated with ZnONPs. **d**

Infected mice treated with L-Camt. **e** Brain tissue of schistosome-infected mice treated with nanoZnO and L-Camt. Bar = 50 μ m

Fig. 4 Effect of ZnONPs and/or L-Carnt treatment to schistosome-infected mice on the brain index. Values are presented as mean \pm SE. ^bSignificance against the infected (Inf) group



the same manner, some reports concluded that gold and selenium nanoparticles showed anti-schistosomal activity in different mice tissues such as the brain, liver, kidney, and spleen (Dkhil et al. 2015b, 2016a, b, 2017).

Moreover, Rani and Panneerselvam (2002) attributed the L-Carnt capacity in prevention of free radical-induced damage to its antioxidant activity. According to Gülcin (2006), L-Carnt scavenges hydrogen peroxide and superoxide radicals, thus protecting the endogenous antioxidant enzymes (CAT) from peroxidative damage and protecting tissues from damage by repairing the oxidized membrane lipids (Alzoubi et al. 2017). Additionally, it exhibits neuroprotective effects on aging animals and neurodegenerative disorders (Rani and Panneerselvam 2002; Shenk et al. 2009). Therefore, Rani and Panneerselvam (2002) reported that L-Carnt supplementation causes a dramatic reduction in the MDA formation and increased the overall antioxidant enzyme status in different brain regions. Also, L-Carnt protects cells from ROS damage by inhibiting free radical propagation and by contributing to the repair of oxidized membrane phospholipid (Arduini 2008). Moreover, Hu et al. (2017) concluded that L-Carnt supplementation reduced inflammation in coronary artery disease due to its antioxidant activity. Therefore, authors decided that L-Carnt high levels could be one of the mechanisms by which *Microtus fortis* mediates protection against *S. japonicum*.

The apoptotic DNA fragmentation was recorded in the brain of schistosome-infected mice. However, the treatment of infected mice with nanoZnO or/and L-Carnt restored DNA laddering profile induced by schistosomiasis. Since schistosomiasis induced oxidative stress (de Oliveira et al. 2013; Bauomy 2014; Dkhil et al. 2015b), and the DNA damage was mediated by ROS (Blair 2008), the oxidative stress could contribute to the degree of DNA fragmentation (Jeng et al. 2015). In addition, the activity of caspase-3, a marker of apoptosis, was estimated in lymphocytes after incubation with the schistosomula (Chen et al. 2002). On the other hand, Shoaie-Hagh et al. (2014) reported that in the isolated rat

pancreatic islets, ZnONPs reduced the apoptosis and oxidative stress. Moreover, Evans and Halliwell (2001) reported that the dietary antioxidants maintained an appropriate antioxidant balance in the case of many infections like malaria.

Concerning the histopathological picture, neuroschistosomiasis caused significant histological impairments that were alleviated by ZnONP or/and L-Carnt injection. These results are in agreement with some studies (Gülcin 2006; Bauomy 2014; Dkhil et al. 2015a, b).

The authors Bauomy (2014) and Dkhil et al. (2015b) reported that neuroschistosomiasis *mansoni* induced significant histological responses in the form of neuronal loss, distortion of the neuronal architecture, disorganization of the pyramidal cells, and nuclear hyperchromasia. In addition, authors observed marked dilated congested blood capillaries as compared with the non-infected control group. However, Dkhil et al. (2015a) deduced that treatment with ZnONPs alleviated the histopathological impairments in the jejunum of mice infected with *Eimeria* sp. and increased the number of goblet cells as compared with the parasite-infected group. Regarding the effect of L-Carnt, Gülcin (2006) reported that it inhibited free radical generation, prevented the impairment of fatty acid beta-oxidation in mitochondria, and protected tissues from damage, by repairing oxidized membrane lipids.

The brain oxidative stress and histopathological impairments in schistosome-infected mice may be explaining the reduced brain index in the present study. However, treatment with L-Carnt increased the brain index as compared with the schistosome-infected group. This increment may be due the antioxidant activity of L-Carnt.

Interestingly, the present study revealed the novel therapeutic potential of ZnONPs, as well as co-treatment of nanoZnO and L-Carnt against neuronal disorders induced by *S. mansoni* infection. NanoZnO and/or L-Carnt treatment reduced the brain levels of oxidative stress, restored DNA laddering profile, and improved the histological distortion. The obtained curative effects

of nanoZnO and L-Carnit are associated with their role as free radical scavengers. Moreover, more investigations are needed to determine the ameliorative cellular mechanisms of nanoparticles on schistosoma-infected mice.

Acknowledgments I would like to thank Prof. Dr. Mohamed Dkhil, Dr. Mona F. Khalil, and Dr. Mohamed Tolba (Zoology Department, Faculty of Science, Helwan University, Egypt) for the help in optimization of some experiments.

Compliance with ethical standards The experiments were approved by state authorities and followed Egyptian rules for animal protection.

Conflict of interest The author declares that there is no conflict of interest.

References

- Abaza SM (2016) Applications of nanomedicine in parasitic diseases. *Parasitol United J* 9(1):1–6
- Abdel-Daim MM, Eissa IAM, Abdeen A, Abdel-Latif HMR, Ismail M, Dawood MAO, Hassan AM (2019) Lycopene and resveratrol ameliorate zinc oxide nanoparticles-induced oxidative stress in Nile tilapia, *Oreochromis niloticus*. *Environ Toxicol Pharmacol* 69:44–50 <https://www.ncbi.nlm.nih.gov/pubmed/30953933>
- Abdelgelil NH, Abdellatif MZM, Abdel-Hafeez EH, Belal US, Mohamed RM, Abdel-Razik AH, Hassanin KMA, Abdel-Wahab A (2019) Effects of iron chelating agent on *Schistosoma mansoni* infected murine model. *Biomed Pharmacother* 109:28–38 <https://www.ncbi.nlm.nih.gov/pubmed/30391706>
- Aebi H (1984) Catalase *in vitro*. *Methods Enzymol* 105:121–126 <https://www.ncbi.nlm.nih.gov/pubmed/6727660>
- Ahmadi F, Ebrahimnejad Y, Ghiasi J, Sis NM (2014) The effect of dietary zinc oxide nanoparticles on the antioxidant state and serum enzymes activity in broiler chickens during starter stage. Presented at: International Conference on Biological, Civil and Environmental Engineering (BCEE-2014) 17–18, Dubai, UAE. <https://doi.org/10.2147/IJN.S79944>
- Aljanabi SM, Martinez I (1997) Universal and rapid salt extraction of high quality genomic DNA for PCR-based techniques. *Nucl Acid Res* 25(22):4692–4693 <https://academic.oup.com/nar/article/25/22/4692/2361305>
- Alzoubi KH, Rababa'h AM, Owaisi A, Khabour OF (2017) L-carnitine prevents memory impairment induced by chronic REM-sleep deprivation. *Br Res Bull* 131:176–182 <https://www.ncbi.nlm.nih.gov/pubmed/28433816>
- Arduini A (2008) Carnitine and its acyl esters as secondary antioxidants? *Ame Heart J* 192(123):1726–1727 <https://www.ncbi.nlm.nih.gov/pubmed/1595568>
- Bauomy AA (2014) The potential role of *Morus Alba* leaves extract on the brain of mice infected with *Schistosoma mansoni*. *CNS Neurol Disord Drug Targets* 13:1513–1519
- Blair IA (2008) DNA adducts with lipid peroxidation products. *J Biol Chem* 283(23):15545–15549 <https://www.jbc.org/content/283/23/15545.full>
- Braga BP, da Costa Junior LB, Lambertucci JR (2003) Magnetic resonance imaging of cerebellar schistosomiasis ansoni. *Rev Soc Bras Med Trop* 36(5):635–636. <https://doi.org/10.1590/S0037-86822003000500018>
- Brevetti G, Perna S (1992) Metabolic and clinical effects of l-carnitine in peripheral vascular disease. In: Ferrari, R., DiMauro, S. and Sherwood, G. (eds.) *L-Carnitine and Its Role in Medicine: From Function to Therapy*. New York: Academic Press, London, pp 359–378
- Chen L, Rao KVN, He YX, Ramaswamy K (2002) Skin-stage Schistosomula of *Schistosoma mansoni* produce an apoptosis-inducing factor that can cause apoptosis of T cells. *J Biol Chem* 277(37):34329–34335 <https://www.ncbi.nlm.nih.gov/pubmed/12107158>
- Chitra K, Annadurai G (2013) Antimicrobial activity of wet chemically engineered spherical shaped ZnO nanoparticles on food borne pathogen. *Int Food Res J* 20(1):59–64
- Coyle CM (2013) Handbook of clinical neurology. In: Schistosomiasis of the nervous system. Vol. 114 (3rd series) *Neuroparasitology and Tropical Neurology*. H.H. Garcia, H.B. Tanowitz, and O.H. Del Brutto, Editors © 2013 Elsevier B.V
- de Oliveira RB, Senger MR, Vasques LM, Gasparotto J, dos Santos JP, Pasquali MA, Moreira JC, Silva FP Jr, Gelain DP (2013) *Schistosoma mansoni* infection causes oxidative stress and alters receptor for advanced glycation end product (RAGE) and tau levels in multiple organs in mice. *Int J Parasit* 43:371–379 <https://www.ncbi.nlm.nih.gov/pubmed/23369670>
- Dkhil MA, Al-Quraishy S, Wahab R (2015a) Anticoccidial and antioxidant activities of zinc oxide nanoparticles on *Eimeria papillata*-induced infection in the jejunum. *Int J Nanomedicine* 10:1961–1968 <https://www.ncbi.nlm.nih.gov/pubmed/25792829>
- Dkhil MA, Bauomy AA, Diab MSM, Wahab R, Delic D, Al-Quraishy S (2015b) Impact of gold nanoparticles on brain of mice infected with *Schistosoma mansoni*. *Parasitol Res* 114(10):3711–3719 <https://www.ncbi.nlm.nih.gov/pubmed/26122996>
- Dkhil MA, Bauomy AA, Diab MSM, Al-Quraishy S (2016a) Protective role of selenium nanoparticles against *Schistosoma mansoni* induced hepatic injury in mice. *Biomed Res* 27(1):214–219
- Dkhil MA, Khalil MF, Bauomy AA, Diab MSM, Al-Quraishy S (2016b) Efficacy of gold nanoparticles against nephrotoxicity induced by *Schistosoma mansoni* infection in mice. *Biomed Environ Sci* 29(11):773–781 <https://www.ncbi.nlm.nih.gov/pubmed/27998383>
- Dkhil MA, Khalil MF, Diab MSM, Bauomy AA, Al-Quraishy S (2017) Effect of gold nanoparticles on mice splenomegaly induced by schistosomiasis mansoni. *SJBS* 24:1418–1423 <https://www.ncbi.nlm.nih.gov/pmc/articles/PMC5562478/>
- Ellman GL (1959) Tissue sulfhydryl groups. *Arch Biochem Biophys* 82(1):70–77 <https://www.ncbi.nlm.nih.gov/pubmed/13650640>
- Emamifar A, Kadivar M, Shahedi M, Soleimani-Zad S (2010) Evaluation of nanocomposite packaging containing Ag and ZnO on shelf life of fresh orange juice. *Innovative Food Sci Emerg Technol* 11:742–748. <https://doi.org/10.1016/j.ifset.2010.06.003>
- Evans P, Halliwell B (2001) Micronutrients: oxidant/antioxidant status. *Br J Nut* 85:S67–S74 <https://www.ncbi.nlm.nih.gov/pubmed/11509092>
- Ferrari TCA, Moreira PRR, Cunha AS (2008) Clinical characterization of neuroschistosomiasis due to *Schistosoma mansoni* and its treatment. *Acta Tropica* 108(2–3):89–97 <https://www.ncbi.nlm.nih.gov/pubmed/18499080>
- Ferrari TCA, Faria LC, Vilaça TS, Correa CR, Góes AM (2011) Identification and characterization of immune complexes in the cerebrospinal fluid of patients with spinal cord schistosomiasis. *J Neuroimmunol* 230(1–2):188–190
- Frederickson CJ, Koh JY, Bush AI (2005) The neurobiology of zinc in health and disease. *Nat Rev Neurosci* 6(6):449–462 <https://www.ncbi.nlm.nih.gov/pubmed/15891778>
- Gandhi PR, Jayaseelan C, Mary RR, Mathivanan D, Suseem SR (2017) Acaricidal, pediculicidal and larvicidal activity of synthesized ZnO nanoparticles using *Momordica charantia* leaf extract against blood feeding parasites. *Exp Parasitol* 181:47e56. <https://doi.org/10.1016/j.exppara.2017.07.007>
- Green LC, Wagner DA, Glogowski J, Skipper PL, Wishnok JS, Tannenbaum SR (1982) Analysis of nitrate, nitrite, and [15N] nitrate

- in biological fluids. *Anal Biochem* 126:131–138. [https://doi.org/10.1016/0003-2697\(82\)90118-x](https://doi.org/10.1016/0003-2697(82)90118-x)
- Gülçin I (2006) Antioxidant and antiradical activities of L-carnitine. *Life Sci* 78:803–811 <https://www.ncbi.nlm.nih.gov/pubmed/16253281>
- Hongfu YBZ (2008) Effects of nano-ZnO on growth performance and diarrhea rate in weaning piglets. *China Feed* 1:008
- Hu Y, Sun L, Yuan Z, XuY CJ (2017) High throughput data analyses of the immune characteristics of *Microtus fortis* infected with *Schistosoma japonicum*. *Sci Rep* 7(1):11311. <https://doi.org/10.1038/s41598-017-11532-2>
- Jeng HA, Pan CH, Chao MR, Lin WY (2015) Sperm DNA oxidative damage and DNA adducts. *Mut Res-Genetic Toxicol Environ Mutagen* 794:75–82. <https://doi.org/10.1016/j.mrgentox.2015.09.002>
- Jin X, Deng M, Kaps S, Zhu X, Hölken I, Mess K, Adelung R, Mishra YK (2014) Study of Tetrapodal ZnO-PDMS composites: a comparison of fillers shapes in stiffness and hydrophobicity improvements. *PLoS One* 9(9):e106991. <https://doi.org/10.1371/journal.pone.0106991>
- Khan YA, Singh BR, Ullah R, Shoeb M, Naqvi AH, Abidi SMA (2015) Anthelmintic effect of biocompatible zinc oxide nanoparticles (ZnONPs) on *Gigantocotyle explanatum*, a neglected parasite of Indian water buffalo. *Pub Lib Sci ONE* 10(7):e0133086. <https://doi.org/10.1371/journal.pone.0133086>
- Kirthi AV, Rahuman AA, Rajakumar G, Marimuthu S, Santhoshkumar T, Jayaseelan C, Velayutham K (2011) Acaricidal, pediculocidal and larvicidal activity of synthesized ZnO nanoparticles using wet chemical route against blood feeding parasites. *Parasitol Res* 109(2):461–472. <https://doi.org/10.1007/s00436-011-2277-8>
- Nadhman A, Nazir S, Khan MI, Arooj S, Bakhtiar M, Shahnaz G, Yasinzaï M (2014) PEGylated silver doped zinc oxide nanoparticles as novel photosensitizers for photodynamic therapy against *Leishmania*. *Free Rad Biol Med* 77:230–238. <https://doi.org/10.1016/j.freeradbiomed.2014.09.005>
- Nazarizadeh A, Asri-Rezaie S (2016) Comparative study of antidiabetic activity and oxidative stress induced by zinc oxide nanoparticles and zinc sulfate in diabetic rats. *AAPS Pharm Sci Tech* 17(4):834–843 <https://link.springer.com/article/10.1208/s12249-015-0405-y>
- Ohkawa H, Ohishi N, Yagi K (1979) Assay for lipid peroxides in animal tissues by thiobarbituric acid reaction. *Anal Biochem* 95:351–358. [https://doi.org/10.1016/0003-2697\(79\)90738-3](https://doi.org/10.1016/0003-2697(79)90738-3)
- Oliver L, Stirewalt MA (1952) An efficient method for the exposure of mice to cercaria of *Schistosoma mansoni*. *J Parasitol* 38:19–23
- Pettegrew JW, Levine J, McClure RJ (2000) Acetyl-L-carnitine physical-chemical, metabolic, and therapeutic properties: relevance for its mode of action in Alzheimer's disease and geriatric depression. *Mol Psych* 5(6):616–632. <https://doi.org/10.1038/sj.mp.4000805>
- Piccinno F, Gottschalk F, Seeger S, Nowack B (2011) Industrial production quantities and uses of ten engineered nanomaterials in Europe and the world. *J Nanopart Res* 14(9):1109–1120. <https://doi.org/10.1007/s11051-012-1109-9>
- Pittella JEH, Gusmão SNS, Carvalho GTC (1996) Tumoral form of cerebral schistosomiasis mansoni: a report of four cases and a review of the literature. *Clinic Neurol Neurosurg* 98:15–20
- Ranasinghe L, Duke M, Harvie M, McManus DP (2018) Kunitz-type protease inhibitor as a vaccine candidate against schistosomiasis mansoni. *Int J Infect Dis* 66:26–32. <https://doi.org/10.1016/j.ijid.2017.10.024>
- Rani PJA, Panneerselvam C (2002) Effect of L-carnitine on brain lipid peroxidation and antioxidant enzymes in old rats. *J Gerontol Series A* 57(4):B134–B137. <https://doi.org/10.1093/gerona/57.4.b134>
- Raso P, Tafuri A, Lopes NF, Monteiro ER, Tafuri WL (2006) The tumoral form of cerebellar schistosomiasis: case report and measure of granulomas. *Rev Soc Bras Med Trop* 39:283–286. <https://doi.org/10.1590/S0037-86822006000300012>
- Reddy KM, Feris K, Bell J, Wingett DG, Hanley C, Punnoose A (2007) Selective toxicity of zinc oxide nanoparticles to prokaryotic and eukaryotic systems. *Appl Phys Lett* 90:2139021–2139023. <https://doi.org/10.1063/1.2742324>
- Sabir S, Arshad M, Chaudhari SK (2014) Zinc oxide nanoparticles for revolutionizing agriculture: synthesis and applications. *Scie World J* 2014:1–8. <https://doi.org/10.1155/2014/925494>
- Saconato H, Atallah A (2000) Interventions for treating schistosomiasis mansoni. *Cochrane Database Systematic Reviews* 2:CD000528. <https://doi.org/10.1002/14651858.CD000528>
- Shenk JC, Liu J, Fischbach K, Xu K, Puchowicz M, Obrenovich ME, Gasimov E, Alvarez LM, Ames BN, Lamanna JC, Aliev G (2009) The effect of acetyl-L-carnitine and R-alpha-lipoic acid treatment in ApoE4 mouse as a model of human Alzheimer's disease. *J Neurol Sci* 283(1–2):199–206. <https://doi.org/10.1016/j.jns.2009.03.002>
- Shoae-Hagh P, Rahimifard M, Navaei-Niggeh M, Baeeri M, Gholami M, Mohammadirad A, Abdollahi M (2014) Zinc oxide nanoparticles reduce apoptosis and oxidative stress values in isolated rat pancreatic islets. *Biol Trace Elem Res* 162(1–3):262–269. <https://doi.org/10.1007/s12011-014-0113-6>
- Siddiqi KS, Ur Rahman A, Tajuddin SM, Husen A (2018) Properties of zinc oxide nanoparticles and their activity against microbes. *Nanos Res Lett* 13:141. <https://doi.org/10.1186/s11671-018-2532-3>
- Slaoui M, Fiette L (2011) Histopathology procedures: from tissue sampling to histopathological evaluation. *Methods Mol Biol* 691:69–82. <https://doi.org/10.1007/978-1-60761-60761-4>
- Tamai I (2013) Pharmacological and pathophysiological roles of carnitine/organic cation transporters (OCTNs: SLC22A4, SLC22A5 and Slc22a21). *Biopharm Drug Dispos* 34:29–44. <https://doi.org/10.1002/bdd.1816>
- Tsakiris S, Schulpis KH, Marinou K, Behrakis P (2004) Protective effect of L-cysteine and glutathione on the modulated suckling rat brain Na⁺, K⁺, -ATPase and Mg²⁺-ATPase activities induced by the *in vitro* galactosaemia. *Pharmacol Res* 49:475–479. <https://doi.org/10.1016/j.phrs.2003.11.006>
- Vrablic AS, Albright CD, Craciunescu CN, Salganik RI, Zeisel SH (2001) Altered mitochondrial function and over generation of reactive oxygen species precede the induction of apoptosis by 1-O-octadecyl-2-methyl-rac-glycero-3-phosphocholine in p53-defective hepatocytes. *Fed Amer Soci Exp Biol J* 15(10):1739–1744. <https://doi.org/10.1096/fj.00-0300com>
- Wahab R, Mishra A, Yun SI, Kim YS, Shin HS (2010) Antibacterial activity of ZnO nanoparticles prepared via non-hydrolytic solution route. *Appl Microbiol Biotechnol* 87(5):1917–1925. <https://doi.org/10.1007/s00253-010-2692-2>
- Xie Y, Wang Y, Zhang T, Ren G, Yang Z (2012) Effects of nanoparticle zinc oxide on spatial cognition and synaptic plasticity in mice with depressive-like behaviors. *J Biomed Sci* 19:14. <https://doi.org/10.1186/1423-0127-19-14>
- Yapar K, Kart A, Karapehlivan M, Atakisi O, Tunca R, Erginsoy S, Cital M (2007) Hepatoprotective effect of L-carnitine against acute acetaminophen toxicity in mice. *Exp Toxicol Pathol* 59(2):121–128. <https://doi.org/10.1016/j.etp.2007.02.009>
- Yu KN, Yoon TJ, Tehrani AM, Kim JE, Park SJ, Jeong MS, Ha SW, Lee JK, Kim JS, Cho MH (2013) Zinc oxide nanoparticle induced autophagic cell death and mitochondrial damage via reactive oxygen species generation. *Toxicol in Vitro* 27:1187–1195. <https://doi.org/10.1016/j.tiv.2013.02.010>
- Zaboli K, Aliarabi H, Bahari A, Abbasalipourkabir R (2013) Role of dietary nano-zinc oxide on growth performance and blood levels of mineral: a study on Iranian Angora (Markhoz) goat kids. *Int Adv Board* 2(1):19–26

Publisher's note Springer Nature remains neutral with regard to jurisdictional claims in published maps and institutional affiliations.